

Quantifying Covalent Interactions with Resonant Inelastic Soft X-ray Scattering: Case Study of Ni²⁺ Aqua Complex

K. Kunnus,^{†,‡} I. Josefsson,[§] S. Schreck,^{†,‡} W. Quevedo,[†] P. S. Miedema,[†] S. Techert,[€]
‡F. M.F. de Groot,[¶] A. Föhlisch,^{†,‡} M. Odelius,[§] Ph. Wernet[†]

[†]*Institute for Methods and Instrumentation for Synchrotron Radiation Research, Helmholtz-Zentrum Berlin für Materialien und Energie GmbH, 12489 Berlin, Germany.*

[‡]*Institut für Physik und Astronomie, Universität Potsdam Karl-Liebknecht-Strasse 24/25
14476 Potsdam, Germany*

[§]*Department of Physics, Stockholm University, AlbaNova University Center, 10691 Stockholm, Sweden*

[€]*Max Planck Institute for Biophysical Chemistry, Am Faßberg 11, 37077 Göttingen, Germany*

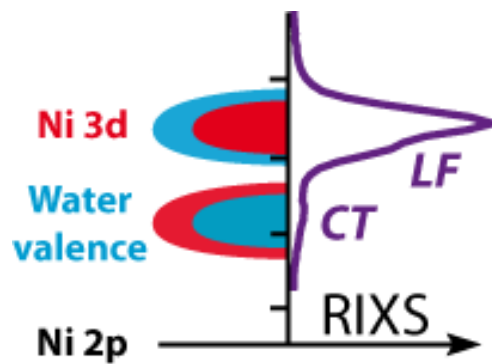
[‡]*Structural Dynamics of (Bio)chemical Systems, DESY, Notkestrasse 85, 22607 Hamburg*

[¶]*Department of Chemistry, Utrecht University, Universiteitsweg 99, 3584 CG Utrecht,
Netherlands*

ABSTRACT

We analyze the effects of covalent interactions in Ni 2p3d resonant inelastic x-ray scattering (RIXS) spectra from aqueous Ni²⁺ ions and find that the relative RIXS intensities of ligand-to-metal charge-transfer final states with respect to the ligand-field final states reflect the covalent mixing between Ni 3d and water orbitals. Specifically, the experimental intensity ratio at the Ni L₃-edge allows to determine that the Ni 3d orbitals have on average 5.5% of water character. Therefore we propose that 2p3d RIXS at the Ni L₃-edge can be utilized to quantify covalency in Ni complexes without the use of external references or simulations.

TOC Graphic:



KEYWORDS: transition-metal ion, aqueous solution, covalent interaction, resonant inelastic x-ray scattering, ligand-field state, charge-transfer state.

INTRODUCTION

Covalency, understood as the sharing of electrons between atomic centers [1], is a fundamental concept that is essential for understanding and predicting basic chemical properties ranging from molecular structures to reactivity and biological function. However, direct experimental determination of covalency, i.e. contributions of atomic orbitals from different atomic centers to a molecular orbital (MO), is generally a difficult task. Here we demonstrate how resonant inelastic x-ray scattering (RIXS) at a 3d transition metal L-edge can be employed to experimentally derive quantitative information on covalent interactions by revealing the atomic compositions of the chemically relevant frontier orbitals. We test our concept by deriving the covalent contributions to the solute-solvent interactions of Ni²⁺ ions in aqueous solution. The interactions of Ni²⁺ with the solvent water molecules can be well described by considering the first solvation shell only [2] with octahedral arrangement of the water ligands. The highly polar coordinative bonding between Ni and the water ligands in the resulting prototypical Werner-type [Ni(H₂O)₆]²⁺ complex is characterized by weak covalent interactions of the ligand-to-metal charge-transfer type ideally serving for a case study [3–5].

Recently, triggered by the development of soft x-ray techniques on liquids and solutions, a number of x-ray absorption spectroscopy (XAS), photoelectron and Auger electron spectroscopy studies have addressed 3d-transition-metal ions in water [2,6–12]. Given the intrinsic sensitivity to local charge distributions, these studies emphasized the covalent effects in metal-solute bonding. This sensitivity of x-ray spectroscopy methods to ligand environment is frequently utilized not only by soft x-ray, but also by hard x-ray techniques [13–18]. However,

quantitative determination of the orbital specific covalent contributions is in practice often beyond the experimental capabilities. Particularly investigations at the transition metal absorption edges require typically elaborate electronic structure calculations and spectral simulations in order to disentangle the inter-atomic covalent effects from intra-atomic and core-hole relaxation effects [8,19–24], although significant advancements with regard to density functional and wavefunction based computational methods have been made in recent years [25–29].

In contrast to sophisticated computational methods, a relatively simple method to derive quantitative information about the metal-ligand covalency from more experimental grounds has been developed by Solomon and co-workers [30]. They derived a formula based on the molecular orbital theory to describe the intensity of ligand K-edge XAS pre-edge feature:

$$I_{XAS} \propto \alpha^2 n_h (1 - k)^2 |\langle \phi_{L1s} | \hat{D} | \phi_{Lnp} \rangle|^2 \quad (1)$$

Here α^2 is metal-ligand covalency (defined as the ligand content in the MO corresponding to the pre-edge feature), n_h is number of holes in the respective MO manifold, k describes the contribution of the other ligand atoms to the MO and the last term is a square of the atomic transition dipole moment. The aim of this this letter is to derive an analogues expression for metal 2p3d RIXS in order to fully exploit the information content embedded in the RIXS spectral intensities.

In our previous experimental work we analyzed in detail the metal-centered ligand-field (LF) RIXS final states at the Ni L_3 and L_2 edge [31]. Crystal field multiplet (CFM) and restricted active

space self-consistent field (RASSCF) calculations presented there did not include ligand-to-metal charge-transfer (LMCT) final states due to computational limitations. In contrast, the present theoretical study concentrates on the LMCT peaks. Our objective is to relate the relative RIXS intensity of LF and LMCT peak to the degree of covalency of the Ni²⁺-water bond, apply it to the experimental spectrum from Ref. [31] and carry out additional charge transfer multiplet (CTM) calculations which include both LF and LMCT final states.

THEORY

RIXS spectra were simulated by multiplying absorption and emission transition moments (two-step approximation) as retrieved from the CTM calculations [32–34]. Exact diagonalization was utilized to calculate the valence- and core-excited states [35]. The following convolution scheme was applied (values for the FWHM are given): 0.35 eV Gaussian broadening taking into account the monochromator bandwidth, 0.5 eV (1.0 eV) Lorentzian lifetime broadening at the L₃ (L₂) edge for core-excited states, and 1.2 eV Gaussian broadening of RIXS spectra to account for the spectrometer resolution. An additional 0.5 eV Gaussian broadening of both x-ray absorption and RIXS spectra was used to account for inhomogeneous broadening. Polarization effects were not included in the simulation of the RIXS spectra (in Ref. [31] we found these are small in horizontal polarization).

RESULTS AND DISCUSSION

Water 3a₁(a_{1g}+e_g+t_{1u}) orbitals are involved in σ-bonding with the Ni 3d(e_g), 4s(a_{1g}) and 4p(t_{1u}) orbitals whereas water 1b₁(t_{2g}+t_{2u}) and Ni 3d(t_{2g}) orbitals exhibit π-interactions in

$[\text{Ni}(\text{H}_2\text{O})_6]^{2+}$. [4,5] The leading covalent contribution has been identified as the mixing between Ni 3d and the water $3a_1$ and $1b_1$ orbitals. [5,36] The most relevant MOs for the present investigation are the bonding (e_g, t_{2g}) nominal ligand and antibonding (e_g^*, t_{2g}^*) nominal Ni MOs as displayed in Figure 1 (a).

The principle of utilizing L-edge RIXS for probing covalency in 3d transition-metal complexes is illustrated in Figure 1 (b) and (c). Resonant excitation to unoccupied nominal Ni 3d MOs at the Ni L-edge is followed by scattering to the LF final states of the $(e_g^*, t_{2g}^*)^8$ configuration or by scattering to the LMCT final states of the $(e_g, t_{2g})^9(e_g^*, t_{2g}^*)^9$ configuration (Figure 1 (b)) [31].

In first approximation the intensities of the LF and LMCT RIXS peaks reflect the Ni 3d composition of the (e_g^*, t_{2g}^*) and (e_g, t_{2g}) MOs, respectively (Figure 1 (c)). Because these MOs are the antibonding and bonding combinations of Ni 3d and water $3a_1$ and $1b_1$ orbitals resulting from the corresponding covalent orbital mixings, the relative intensities of LF and LMCT RIXS peaks can be expected to correlate with the magnitude of these mixings, i.e. the covalency in the complex.

The qualitative considerations outlined above are scrutinized as follows. Within the framework of LCAO-MO theory the covalent bonding between atoms is described in terms of mixing of atomic orbitals at different atomic sites. In case of metal-centered complexes such as $[\text{Ni}(\text{H}_2\text{O})_6]^{2+}$ we can describe the bonding between the metal and the ligands as a mixing of the symmetry adapted metal orbitals with ligand group orbitals (LGO) formed by a symmetry adapted mixing of the equivalent ligand orbitals. Mixing of one metal orbital with one LGO results in a pair of bonding and antibonding MOs:

$$\psi = \alpha\phi_M + \sqrt{1 - \alpha^2}\phi_L$$

$$\psi^* = \sqrt{1 - \alpha^2}\phi_M - \alpha\phi_L$$

where ψ is a bonding and ψ^* an antibonding MO, ϕ_M is an atomic metal orbital and ϕ_L is a LGO. The parameter α^2 describes the magnitude of mixing between the metal orbital and the LGO and can be interpreted as the relative contribution of ligand orbitals to the antibonding MO (or the relative amount of metal orbitals in the bonding MO). We have followed here the same definition of covalency as used by Solomon et al [19,30].

Within approximations detailed below (most importantly the one-electron and the frozen-orbital approximations), the dipole transition matrix elements involving decay from the ψ and ψ^* MOs to an atomic metal 2p core orbital ϕ_{M2p} can be written as:

$$|\langle\psi|\widehat{D}|\phi_{M2p}\rangle|^2 = \alpha^2|\langle\phi_{M3d}|\widehat{D}|\phi_{M2p}\rangle|^2 \quad (2)$$

$$|\langle\psi^*|\widehat{D}|\phi_{M2p}\rangle|^2 = (1 - \alpha^2)|\langle\phi_{M3d}|\widehat{D}|\phi_{M2p}\rangle|^2$$

Where ϕ_{M3d} is a metal 3d orbital, ϕ_{M2p} is a metal 2p core orbital and D is the dipole transition operator. The above equations indicate that the transition probabilities are proportional to the 3d character of the respective orbitals. To describe the relative RIXS intensities, the number and occupation of the ψ and ψ^* MOs in the core-excited states has to be taken into account in addition. In case of $[\text{Ni}(\text{H}_2\text{O})_6]^{2+}$ we must consider the two sets of bonding and antibonding orbitals (e_g, e_g^*) and (t_{2g}, t_{2g}^*) with different covalency that we define as α_{Eg}^2 and α_{T2g}^2 . The occupation of these orbitals in the core-excited states is evident from the electronic

configurations of the core-excited states, namely $(2p)^5(e_g)^4(t_{2g})^6(t_{2g}^*)^6(e_g^*)^3$. The relative intensities of LF and LMCT RIXS peaks is thus

$$\frac{I_{LMCT}}{I_{LF}} = \frac{4\alpha_{Eg}^2 + 6\alpha_{T2g}^2}{3(1-\alpha_{Eg}^2) + 6(1-\alpha_{T2g}^2)} \quad (3)$$

To experimentally determine the average covalency we introduce the weighted average $\langle\alpha^2\rangle = (4/10) \cdot \alpha_{Eg}^2 + (6/10) \cdot \alpha_{T2g}^2$ to describe the overall mixing of the nominal metal 3d with the water orbitals. From Equation (3) now one can derive an approximate relation for the average covalency for the $[\text{Ni}(\text{H}_2\text{O})_6]^{2+}$ complex:

$$\langle\alpha^2\rangle = \frac{9\frac{I_{LMCT}}{I_{LF}}}{9\frac{I_{LMCT}}{I_{LF}} + 10} \quad (4)$$

Within the given approximations it is thus evident that the average 3d covalency of the $[\text{Ni}(\text{H}_2\text{O})_6]^{2+}$ complex is given by the relative intensity of LMCT with respect to LF peaks in the Ni L-edge RIXS spectrum, without any additional theoretical simulations. The experimental requirement is that the LF and LMCT RIXS peaks can be separated in the spectrum and their intensities determined.

The experimental Ni L_3 -edge RIXS spectra of $\text{Ni}^{2+}(\text{aq})$ from Ref. [31] are displayed in Figure 2(a), with clearly resolved LF and CT RIXS features. The $\text{Ni}^{2+}(\text{aq})$ L-edge x-ray absorption spectrum is well known [7,25,31,37]. The two LF peaks at energy transfers of 1.1 and 3.7 eV can be assigned to a number of unresolved valence-excited LF states of the $(e_g^*, t_{2g}^*)^8$ configuration and the broad peak at 9.5 eV corresponds to the LMCT final states of the $(e_g, t_{2g})^9(e_g^*, t_{2g}^*)^9$

configuration.[31] In order to determine the relative intensities of the LF and LMCT peaks $I_{\text{LMCT}}/I_{\text{LF}}$ we integrate the RIXS intensities for incident photon energies of the L_3 absorption edge (from 850-858 eV, Figure 2(b)). $I_{\text{LMCT}}/I_{\text{LF}}$ is then determined from fitting this integrated spectrum (Figure 2(b)) and we find $I_{\text{LMCT}}/I_{\text{LF}} = 0.065$. With Equation (4) we determine the average ground-state covalency of the Ni-water bond in the $[\text{Ni}(\text{H}_2\text{O})_6]^{2+}$ complex to 0.055 implying that the Ni 3d-dominated antibonding frontier orbitals have on average 5.5% of water-ligand character. The question occurs about how valid this concept is in general and for evaluating this we proceed to discussing the validity of the approximations introduced to derive Equation (4).

First, Equation (4) neglects multi-electron correlation (multiplet) effects, namely the 2p-3d and 3d-3d Coulomb interactions and the 2p and 3d spin-orbit interaction. We therefore assumed that the LF and LMCT features in the integrated RIXS spectrum of the complex can be assigned within the one-electron model by describing the corresponding RIXS final states with single determinants. However it is well-known that multiplet effects have to be accounted for when describing shapes and energies of L-edge RIXS of transition-metal complexes [32,38] and this is also evident from the multiplet structure in Figure 2 (a). It is thus somewhat surprising that their exclusion should yield a valid description. Second, the frozen-orbital approximation is applied in a sense that the inter-atomic core-hole screening is neglected and, therefore, the covalency α^2 is the same for ground and core-excited states. The validity of these two approximations is addressed below and we find *a posteriori* that the approximations are justified for the case studied here. Note that we implicitly also employ the local approximation as routinely used to interpret XAS and RIXS data [39,40] by discarding all non-local contributions to the RIXS intensities, i.e. contributions which arise from transitions of different

atomic sites than the core-excited Ni site. In addition, we omit channel interference by assuming that independent absorption and emission steps can describe the RIXS process. Although interference between different resonant scattering channels is generally necessary to describe L-edge RIXS of 3d transition-metal ions[41], we have showed in Ref. [31] that the two step approximation is valid at the Ni L-edge of $[\text{Ni}(\text{H}_2\text{O})_6]^{2+}$ at both the L_3 and L_2 edges.

We address the one-electron and frozen-orbital approximations by performing a series of calculations using the well-established CTM model and the corresponding calculated spectra are compared to experiment in Figure 2 (c). The multiplet effects were included in a standard scheme where for the 2p-3d and 3d-3d Coulomb interaction terms Hartree-Fock atomic values scaled by 0.9 were used and for the 2p and 3d spin-orbit interactions the unscaled Hartree-Fock atomic values were used. In the CTM calculations, covalent interactions in $[\text{Ni}(\text{H}_2\text{O})_6]^{2+}$ with nominal d^8 configuration are accounted for by an Anderson impurity model by coupling the states originating from $3d^8$ and ligand (L)-to-metal LMCT $3d^9L^{-1}$ configurations [42–44]. The extent of coupling is controlled by the charge transfer energy Δ_g (difference between the average energies of the $3d^8$ and $3d^9L^{-1}$ multiplets) and by the mixing parameters T (non-diagonal elements of the Hamiltonian). For the calculations of the spectra in Figure 2 (c) the mixing parameters were set to $T(E_g) = 2.0$ eV and $T(T_{2g}) = 1.0$ eV and were kept the same also for the core-excited states. These values are typical for weakly covalent transition metal oxide compounds in local octahedral symmetry [32,45]. The RIXS final state energies are uniquely determined by the multiplet interactions in the $3d^8$ configuration, the charge transfer energy Δ_g , and the mixing parameters $T(E_g)$ and $T(T_{2g})$. The value for Δ_g of 6.5 eV was thus chosen to be the experimental separation of LF and LMCT energies. The core-hole relaxation effect can be

simulated in the CTM model by using different values for the charge transfer energy Δ_c for the respective core-excited configurations $2p^5d^9$ and $2p^5d^{10}L^{-1}$. A difference of the charge transfer energies in the ground and core-excited states, $\Delta_c - \Delta_g$, is a resultant effect of the 2p core-hole potential U_{pd} and the valence electron repulsion U_{dd} caused by the addition of an extra electron to the 3d manifold. It has been shown that in 3d transition-metal compounds U_{pd} is larger than U_{dd} by typically 1-2 eV and, therefore, at the L-edge $-1 \text{ eV} > \Delta_c - \Delta_g > -2 \text{ eV}$ [32]. Given this parameter space we performed three CTM calculations, defined by the parameter sets given in Table 1 with the corresponding spectra displayed in Figure 2 (c). As for the experimental spectra, the calculated spectra in Figure 2 (c) result from integrating the calculated RIXS intensities for incident photon energies across the L_3 absorption edge. We display in Figure 3 the calculated L-edge RIXS intensities versus energy transfer and incident photon energy.

For the CTM calculation with multiplet and core-hole relaxation effects [“CTM”, Figure 3 (a) and red line in Figure 2 (c)] we find $I_{LMCT}/I_{LF} = 0.066$ in excellent agreement with experiment. Without core-hole relaxation this is smaller by 6% ($I_{LMCT}/I_{LF} = 0.062$) and the spectral shapes of both the integrated RIXS spectrum (“CTM no relax.”, green line in Figure 2 (c)) and of the full RIXS plane (Figure 3 (b)) remain largely unchanged. The core-hole relaxation effect slightly increases I_{LMCT}/I_{LF} (Figure 2 (c)) because lowering of Δ_c with respect to Δ_g increases covalent mixing between the core-excited configurations. We thus find that in the case of $[\text{Ni}(\text{H}_2\text{O})_6]^{2+}$ the core-hole relaxation has only a minor influence on I_{LMCT}/I_{LF} (because $\Delta_g > T$ and $\Delta_c > T$) and as a consequence the core-hole induced change of covalency is small. We note that a so-called charge-transfer satellite peak in the x-ray absorption spectrum of 3d transition metals was shown to be proportional to the change in mixing between $3d^n$ and $3d^{n+1}L^{-1}$ configurations [46].

Such a satellite peak is experimentally not detectable in the x-ray absorption spectrum of $\text{Ni}^{2+}(\text{aq})$, independently confirming that the core-hole relaxation influences the covalency in the core-excited states to a minor degree only. The influence of core-hole relaxation on charge transfer could be further adjusted by lowering the mixing parameters in the core-excited configuration to model the effect of radial contraction of the Ni orbitals due to positively charged core-hole [46]. Contrary to the effect of lowering Δ_c respect to Δ_g , this would decrease the $I_{\text{LMCT}}/I_{\text{LF}}$. We have left here the mixing parameters unchanged because the CTM calculation with multiplet and core-hole relaxation effects already reproduces very well the experimental observable $I_{\text{LMCT}}/I_{\text{LF}}$. The measured shape of the LMCT feature is not well reproduced in the CTM calculation. This can be explained by the various ligand-orbital energies being approximated by a single parameter Δ_g . In the third (“CTM, no relax., only 2p SO”) and fourth calculation [“CTM no relax., no mult.”, Figure 3 (c) and blue line in Figure 2 (c)] both multiplet and core-hole relaxation effects were turned off. The fourth calculation is thus performed at the same level of approximations as used for deriving Equations (3) and (4). As expected, the shape of the calculated RIXS plane changes drastically and has no resemblance with the full calculation including all relevant effects (Figure 3). Interestingly, however, the calculated integrated RIXS spectrum still shows acceptable agreement with the measured integrated RIXS spectrum (Figure 2). Even more notably, the calculated $I_{\text{LMCT}}/I_{\text{LF}}$ ratio of 0.066 does not change compared to the calculation including both multiplet and core-hole relaxation effects. It is likely coincidental that the multiplet effects so exactly balance out the core-hole relaxation effects in the current case. This is suggested by the comparison with calculated results at the L2 edge which show systematically higher $I_{\text{LMCT}}/I_{\text{LF}}$ ratios (Table 2). Nevertheless, it is clear that the

multiplet effects have also only a small influence on the $I_{\text{LMCT}}/I_{\text{LF}}$ ratio. Our calculations therefore demonstrate that the one-electron approximation and the frozen-orbital approximation used to derive Equations (3) and (4) are well justified in case of $[\text{Ni}(\text{H}_2\text{O})_6]^{2+}$. All calculated $I_{\text{LMCT}}/I_{\text{LF}}$ ratios and the corresponding average covalencies $\langle\alpha^2\rangle$ with Equation (4) are compared to experiment in Table 2. It will be interesting in future studies to compare the experimentally derived values for the Ni^{2+} - H_2O covalency with calculated values. In addition, the concept presented here could be further tested on other 3d transition metal ions in water thereby systematizing how multiplet and core-hole relaxation effects influence the RIXS spectra and the derived covalency.

SUMMARY AND CONCLUSIONS

Summarizing, we showed that the relative intensity of LMCT and LF spectral features in the Ni L-edge resonant inelastic x-ray scattering spectrum of the hexaaqua complex $[\text{Ni}(\text{H}_2\text{O})_6]^{2+}$ is dominantly determined by the ground state covalent mixing between the Ni 3d orbitals and the water-ligand orbitals. Based on a derived relationship of this intensity ratio and the ground-state covalency accounting for the occupation of the respective molecular orbitals allows us to derive the average covalent contribution to the Ni^{2+} solute and water solvent interactions. We arrive at 0.055 meaning that the nominal Ni 3d antibonding molecular orbitals have an average of 5.5% of ligand H_2O $1b_1$ and $3a_1$ character. This represents a stringent test for modern quantum chemistry approaches. We consider it possible that the conclusions drawn here are valid not only for weakly covalent Ni^{2+} complexes, but potentially also for complexes with different metals, oxidations states and higher covalency.

Tables and Figures

Table 1. Parameters used for scaling the 2p-3d and 3d-3d Coulomb and 2p and 3d spin-orbit interactions and the ground (Δ_g) and core-excited state (Δ_c) charge transfer energies in the CTM calculations of Ni L₃-RIXS of $[\text{Ni}(\text{H}_2\text{O})_6]^{2+}$. The ligand field strength 10Dq was set to 1.1 eV and the mixing parameters were set to $T(E_g) = 2.0$ eV and $T(T_{2g}) = 1.0$ eV for ground and core-excited states. See text for more details.

	Scaling of Coulomb interactions	Scaling of 2p spin-orbit interactions	Scaling of 3d spin-orbit interactions	Δ_g	Δ_c
CTM	0.9	1	1	6.5	5.5
CTM, no relax.	0.9	1	1	6.5	6.5
CTM, no relax., only 2p SO	0	1	0	6.5	6.5
CTM, no relax., no mult.	0	0	0	6.5	6.5

Table 2. Measured and calculated relative intensities of charge-transfer and ligand-field Ni L₃-RIXS features $I_{\text{LMCT}}/I_{\text{LF}}$ in $[\text{Ni}(\text{H}_2\text{O})_6]^{2+}$ and the corresponding values for the average covalency $\langle \alpha^2 \rangle$ following from Equation (4).

	$I_{\text{LMCT}}/I_{\text{LF}}$			$\langle \alpha^2 \rangle$		
	L ₃	L ₂	L _{2,3}	L ₃	L ₂	L _{2,3}
Expt.	0.065	-	-	0.055	-	-
CTM	0.066	0.077	0.074	0.056	0.065	0.062
CTM, no relax.	0.062	0.075	0.068	0.053	0.063	0.058
CTM, no relax., only 2p SO	0.059	0.062	0.060	0.050	0.053	0.051
CTM, no relax., no mult.	-	-	0.066	-	-	0.056

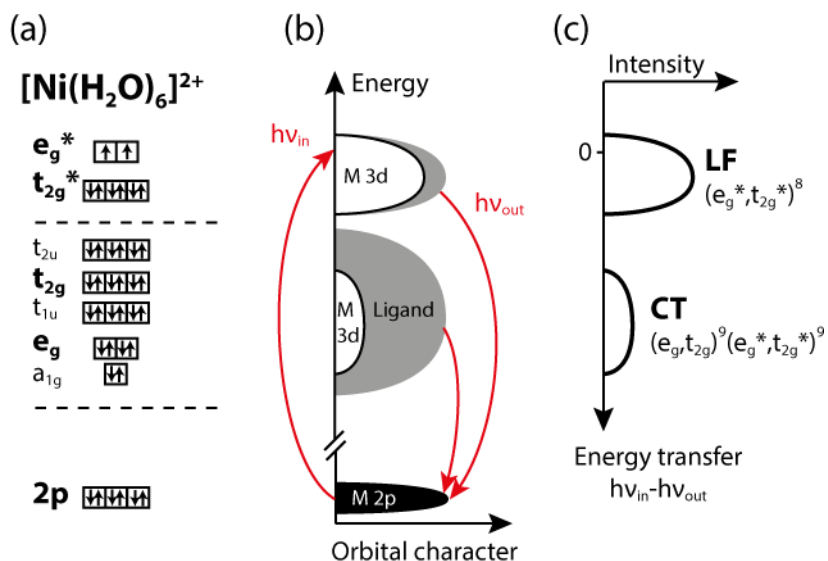


Figure 1. (a) Schematic molecular orbital (MO) diagram for the hexaaqua $[\text{Ni}(\text{H}_2\text{O})_6]^{2+}$ complex. Bold letters are used for the orbitals relevant for the present investigation. e_g/e_g^* and t_{2g}/t_{2g}^* MOs form two sets of bonding/antibonding orbitals, governing the covalent interaction. (b) Schematic depiction of the resonant inelastic x-ray scattering (RIXS) process in a transition-metal complex. The metal 3d and ligand characters of the MOs are shown in white and grey, respectively. For $[\text{Ni}(\text{H}_2\text{O})_6]^{2+}$ these are Ni 3d and water $3a_1/1b_1$ characters in the nominal metal e_g^* and t_{2g}^* and nominal ligand e_g and t_{2g} MOs. $h\nu_{in}$ and $h\nu_{out}$ denote the incident and the emitted photon energies. (c) Schematic RIXS spectrum with RIXS intensities versus energy transfer. The peak denoted LF corresponds to RIXS final states assigned to valence-excited ligand-field states [states of the $(e_g^*, t_{2g}^*)^8$ configuration for $\text{Ni}^{2+}(\text{aq})$] and the peak denoted CT corresponds to RIXS final states assigned to ligand-to-metal charge-transfer states [$(e_g, t_{2g})^9(e_g^*, t_{2g}^*)^9$ configuration for $\text{Ni}^{2+}(\text{aq})$]. The intensities of LF and CT peaks reflect the metal 3d (Ni 3d) character of the MOs [(e_g^*, t_{2g}^*) and (e_g, t_{2g})].

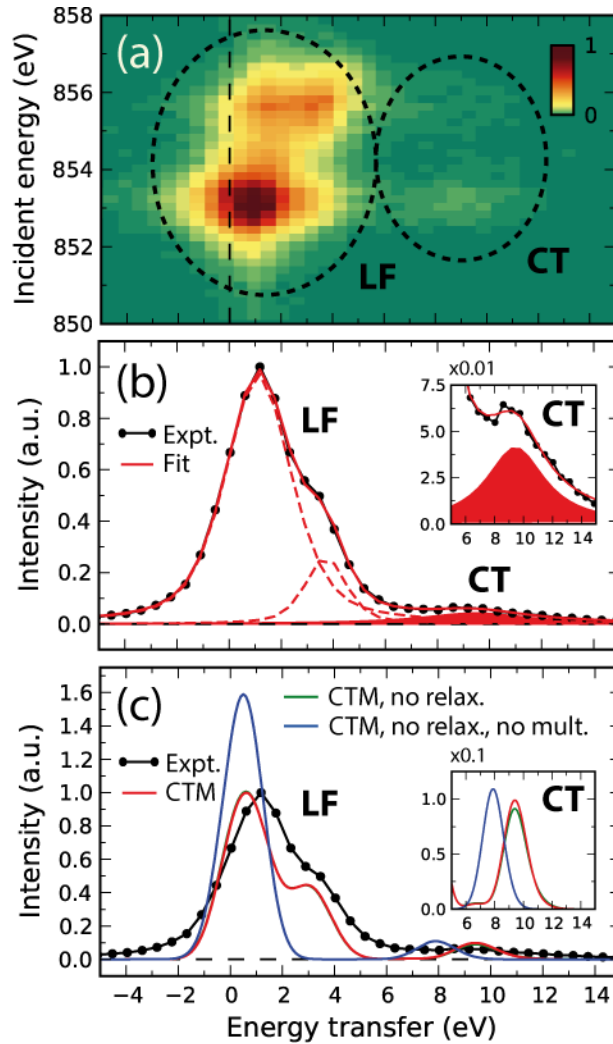


Figure 2. (a) Experimental RIXS intensities of $\text{Ni}^{2+}(\text{aq})$ at the Ni L_3 -edge encoded in color versus energy transfer and incident photon energy. Spectral features denoted with LF and CT correspond to ligand-field and charge-transfer excited states, respectively. (b) Filled circles with solid black line: Measured RIXS intensities versus energy transfer resulting from integrating all intensities in (a) over the displayed incident-photon-energy range (normalized to one at maximum). Solid red line: Fit of a sum of three pseudo-Voigt profiles (dashed red lines) to the measured data. The CT peak at an energy transfer of 9.5 eV is highlighted by the filled red pseudo-Voigt profile and on an enlarged scale in the inset. According to the fit, the area of the CT peak divided by the total area of the LF features equals 0.065. (c) Solid red line: Result of a charge-transfer multiplet (CTM) calculation including electron correlation (multiplet) and core-hole relaxation effects. Solid green line: CTM calculation including multiplet but no core-hole effects (frozen-orbital approximation, the line is barely visible as it is nearly identical to the red one, see the inset for differences). Solid blue line: CTM calculation without multiplet and core-hole relaxation effects (one-electron and frozen-orbital approximation). Filled circles with solid black line: Measured data, same as in (b). For details of the CTM calculations see text and Table 1.

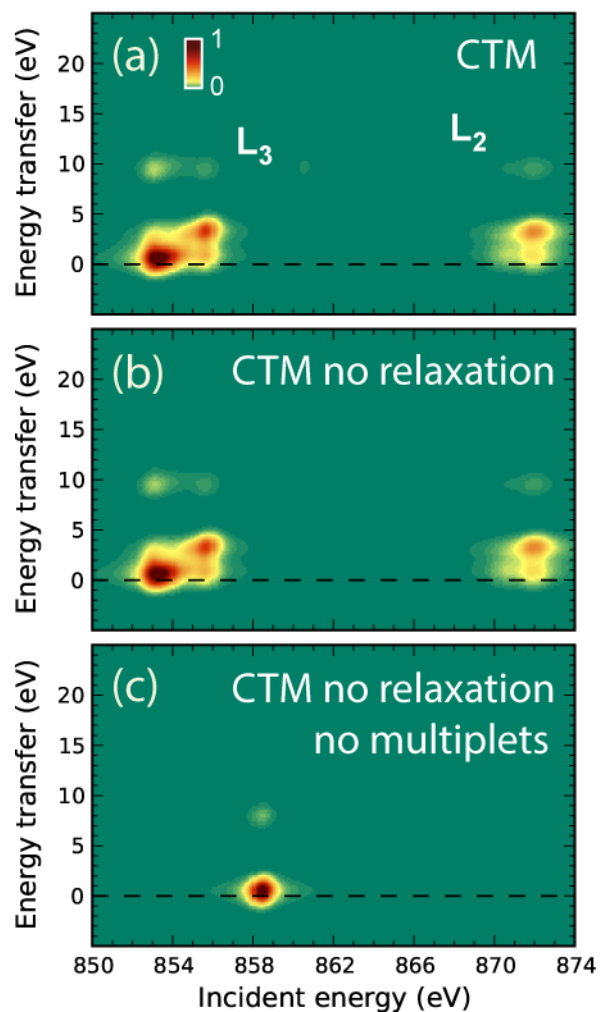


Figure 3. Calculated $\text{Ni}^{2+}(\text{aq})$ RIXS intensities over the whole Ni $L_{2,3}$ -edge. (a) CTM calculation including electron-correlation (multiplet) and core-hole relaxation effects (“CTM”), (b) CTM calculation including multiplet but no core-hole relaxation effects (frozen-orbital approximation, “CTM no relaxation”). (c) CTM calculation without multiplet and core-hole relaxation effects (one-electron and frozen-orbital approximation, “CTM no relaxation, no multiplets”).

AUTHOR INFORMATION

Corresponding Author

*E-mail: kkunnus@stanford.edu, Phone: +1 (650) 926-3906

ACKNOWLEDGMENTS

K.K. acknowledges Thomas Kroll for fruitful discussions. M.O. acknowledges financial support from the Swedish Research Council and Carl Tryggers foundation. We gratefully acknowledge the continuous support by the BESSY II staff and we thank HZB for the allocation of synchrotron radiation beamtime. Portions of the presented research were funded by the Helmholtz Virtual Institute “Dynamic Pathways in Multidimensional Landscapes”.

References

- [1] G.N. Lewis, *The Atom and the Molecule*, *J. Am. Chem. Soc.* 38 (1916) 762–785.
- [2] L.A. Näslund, M. Cavalleri, H. Ogasawara, A. Nilsson, L.G.M. Pettersson, P. Wernet, et al., Direct evidence of orbital mixing between water and solvated transition-metal ions: An oxygen 1s XAS and DFT study of aqueous systems, *J. Phys. Chem. A* 107 (2003) 6869–6876. doi:10.1021/jp034296h.
- [3] A. Werner, *Beitrag zur Konstitution anorganischer Verbindungen*, *Zeitschrift Für Anorg. Chemie.* 3 (1893) 267–330.
- [4] B.N. Figgis, M.A. Hitchman, *Ligand Field Theory and Its Applications*, Wiley-VCH, 2000.
- [5] R. Åkesson, L.G.M. Pettersson, M. Sandstrom, U. Wahlgren, Ligand-field effects in the hydrated divalent and trivalent metal-ions of the first and 2nd transition periods, *J. Am. Chem. Soc.* 116 (1994) 8691–8704.
- [6] S. Bonhommeau, N. Ottosson, W. Pokapanich, S. Svensson, W. Eberhardt, O. Bjorneholm, et al., Solvent effect of alcohols at the {L-edge} of iron in solution: X-ray absorption and multiplet calculations, *J. Phys. Chem. B* 112 (2008) 12571–12574. doi:10.1021/jp8071266.
- [7] E.F. Aziz, The solvation of ions and molecules probed via soft X-ray spectroscopies, *J. Electron Spectrosc. Relat. Phenom.* 177 (2010) 168–180. doi:10.1016/j.elspec.2010.02.009.
- [8] P. Wernet, K. Kunnus, S. Schreck, W. Quevedo, R. Kurian, S. Techert, et al., Dissecting local atomic and intermolecular interactions of transition-metal ions in solution with selective X-ray spectroscopy, *J. Phys.*

- Chem. Lett. 3 (2012) 3448–3453.
- [9] K. Atak, S.I. Bokarev, M. Gotz, R. Golnak, K.M. Lange, N. Engel, et al., Nature of the Chemical Bond of Aqueous Fe^{2+} Probed by Soft X-ray Spectroscopies and ab Initio Calculations, *J. Phys. Chem. B.* 117 (2013). doi:10.1021/jp408212u.
- [10] B. Winter, M. Faubel, Photoemission from liquid aqueous solutions, *Chem. Rev.* 106 (2006) 1176–1211. doi:10.1021/cr040381p.
- [11] S. Thürmer, R. Seidel, W. Eberhardt, S.E. Bradforth, B. Winter, Ultrafast Hybridization Screening in Fe^{3+} Aqueous Solution, *J. Am. Chem. Soc.* 133 (2011) 12528–12535. doi:10.1021/ja200268b.
- [12] R. Golnak, S.I. Bokarev, R. Seidel, J. Xiao, G. Grell, K. Atak, et al., Joint Analysis of Radiative and Non-Radiative Electronic Relaxation Upon X-ray Irradiation of Transition Metal Aqueous Solutions, *Sci. Rep.* 6 (2016) 24659. doi:10.1038/srep24659.
- [13] U. Bergmann, C.R. Horne, T.J. Collins, J.M. Workman, S.P. Cramer, Chemical dependence of interatomic X-ray transition energies and intensities – a study of Mn $K\beta''$ and $K\beta_{2,5}$ spectra, *Chem. Phys. Lett.* 302 (1999) 119–124. doi:10.1016/S0009-2614(99)00095-0.
- [14] N. Lee, T. Petrenko, U. Bergmann, F. Neese, S. DeBeer, Probing Valence Orbital Composition with Iron $K\beta$ X-ray Emission Spectroscopy, *J. Am. Chem. Soc.* 132 (2010) 9715–9727. doi:10.1021/ja101281e.
- [15] D.A. Meyer, X. Zhang, U. Bergmann, K.J. Gaffney, Characterization of charge transfer excitations in hexacyanomanganate(III) with Mn K-edge resonant inelastic x-ray scattering., *J. Chem. Phys.* 132 (2010) 134502. doi:10.1063/1.3367958.
- [16] C.J. Pollock, M.U. Delgado-Jaime, M. Atanasov, F. Neese, S. DeBeer, $K\beta$ mainline X-ray emission spectroscopy as an experimental probe of metal-ligand covalency., *J. Am. Chem. Soc.* 136 (2014) 9453–63. doi:10.1021/ja504182n.
- [17] M.A. Beckwith, M. Roemelt, M.-N. Collomb, C. DuBoc, T.-C. Weng, U. Bergmann, et al., Manganese $K\beta$ X-ray emission spectroscopy as a probe of metal-ligand interactions., *Inorg. Chem.* 50 (2011) 8397–409. doi:10.1021/ic200970t.
- [18] M. Lundberg, T. Kroll, S. Debeer, U. Bergmann, S. a. Wilson, P. Glatzel, et al., Metal-ligand covalency of iron complexes from high-resolution resonant inelastic X-ray scattering, *J. Am. Chem. Soc.* 135 (2013) 17121–17134.
- [19] † Erik C. Wasinger, ‡ Frank M. F. de Groot, *,†,§ Britt Hedman, *,†,§ and Keith O. Hodgson, † Edward I. Solomon*, L-edge X-ray Absorption Spectroscopy of Non-Heme Iron Sites: Experimental Determination of Differential Orbital Covalency, (2003). doi:10.1021/JA034634S.
- [20] R.K. Hocking, E.C. Wasinger, F.M.F. de Groot, K.O. Hodgson, B. Hedman, E.I. Solomon, Fe L-edge XAS studies of $K_4[\text{Fe}(\text{CN})_6]$ and $K_3[\text{Fe}(\text{CN})_6]$: A direct probe of back-bonding, *J. Am. Chem. Soc.* 128 (2006) 10442–10451. doi:10.1021/ja061802i.
- [21] E. Suljoti, R. Garcia-Diez, S.I. Bokarev, K.M. Lange, R. Schoch, B. Dierker, et al., Direct observation of

- molecular orbital mixing in a solvated organometallic complex, *Angew. Chemie - Int. Ed.* 52 (2013) 9841–9844. doi:10.1002/anie.201303310.
- [22] N. Engel, S.I. Bokarev, E. Suljoti, R. Garcia-Diez, K.M. Lange, K. Atak, et al., Chemical bonding in aqueous ferrocyanide: Experimental and theoretical X-ray spectroscopic study, *J. Phys. Chem. B.* 118 (2014) 1555–1563. doi:10.1021/jp411782y.
- [23] T. Kroll, E.I. Solomon, F.M.F. de Groot, Final-State Projection Method in Charge-Transfer Multiplet Calculations: An Analysis of Ti L-Edge Absorption Spectra, *J. Phys. Chem. B.* 119 (2015) 13852–13858. doi:10.1021/acs.jpccb.5b04133.
- [24] K. Kunnus, W. Zhang, M.G. Delcey, R. V. Pinjari, P.S. Miedema, S. Schreck, et al., Viewing the Valence Electronic Structure of Ferric and Ferrous Hexacyanide in Solution from the Fe and Cyanide Perspectives, (2016).
- [25] I. Josefsson, K. Kunnus, S. Schreck, A. Föhlisch, F. De Groot, P. Wernet, et al., Ab initio calculations of X-ray spectra: Atomic multiplet and molecular orbital effects in a multiconfigurational scf approach to the L-edge spectra of transition metal complexes, *J. Phys. Chem. Lett.* 3 (2012) 3565–3570. doi:10.1021/jz301479j.
- [26] M. Roemelt, D. Maganas, S. DeBeer, F. Neese, A combined {DFT} and restricted open-shell configuration interaction method including spin-orbit coupling: Application to transition metal {L}-edge X-ray absorption spectroscopy, *J. Chem. Phys.* 138 (2013) 204101.
- [27] S.I. Bokarev, M. Dantz, E. Suljoti, O. Kühn, E.F. Aziz, State-dependent electron delocalization dynamics at the solute-solvent interface: Soft-x-ray absorption spectroscopy and Ab initio calculations, *Phys. Rev. Lett.* 111 (2013) 83002. doi:10.1103/PhysRevLett.111.083002.
- [28] R. V Pinjari, M.G. Delcey, M. Guo, M. Odelius, M. Lundberg, Restricted active space calculations of L-edge X-ray absorption spectra: from molecular orbitals to multiplet states., *J. Chem. Phys.* 141 (2014) 124116. doi:10.1063/1.4896373.
- [29] M. Preuß, S.I. Bokarev, S.G. Aziz, O. Kühn, Towards an ab initio theory for metal L-edge soft X-ray spectroscopy of molecular aggregates, *Struct. Dyn.* 3 (2016) 62601. doi:10.1063/1.4961953.
- [30] E.I. Solomon, B. Hedman, K.O. Hodgson, A. Dey, R.K. Szilagy, Ligand K-edge X-ray absorption spectroscopy: covalency of ligand–metal bonds, *Coord. Chem. Rev.* 249 (2005) 97–129. doi:10.1016/j.ccr.2004.03.020.
- [31] K. Kunnus, I. Josefsson, S. Schreck, W. Quevedo, P.S. Miedema, S. Techert, et al., From ligand fields to molecular orbitals: Probing the local valence electronic structure of Ni²⁺ in aqueous solution with resonant inelastic X-ray scattering, *J. Phys. Chem. B.* 117 (2013) 16512–16521. doi:10.1021/jp4100813.
- [32] F.M.F. de Groot, A. Kotani, *Core Level Spectroscopy of Solids*, CRC Press, Boca Raton, 2008.
- [33] B.T. Thole, G. van der Laan, J.C. Fuggle, G.A. Sawatzky, R.C. Karnatak, J.-M. Esteva, 3d x-ray-absorption lines and the 3d⁹fn+1 multiplets of the lanthanides, *Phys. Rev. B.* 32 (1985) 5107–5118. doi:10.1103/PhysRevB.32.5107.
- [34] F.M.F. de Groot, J.C. Fuggle, B.T. Thole, G.A. Sawatzky, 2p X-Ray Absorption Of 3d Transition-Metal

- Compounds - An Atomic Multiplet Description Including The Crystal-Field, *Phys. Rev. B.* 42 (1990) 5459–5468. doi:10.1103/PhysRevB.42.5459.
- [35] R.J. Green, D.A. Zatsepin, D.J. St. Onge, E.Z. Kurmaev, N. V. Gavrilov, A.F. Zatsepin, et al., Electronic band gap reduction and intense luminescence in Co and Mn ion-implanted SiO₂, *J. Appl. Phys.* 115 (2014) 103708. doi:10.1063/1.4868297.
- [36] B. Kallies, R. Meier, Electronic structure of 3d M(H₂O)₆³⁺ ions from Sc-III to Fe-III: A quantum mechanical study based on DFT computations and natural bond orbital analyses, *Inorg. Chem.* 40 (2001) 3101–3112. doi:10.1021/ic001258t.
- [37] R. Seidel, S. Thürmer, B. Winter, Photoelectron Spectroscopy Meets Aqueous Solution: Studies from a Vacuum Liquid Microjet, *J. Phys. Chem. Lett.* 2 (2011) 633–641. doi:10.1021/jz101636y.
- [38] F.M.F. de Groot, Multiplet effects in X-ray spectroscopy, *Coord. Chem. Rev.* 249 (2005) 31–63. doi:10.1016/j.ccr.2004.03.018.
- [39] J. Stöhr, *NEXAFS Spectroscopy*, Springer, Berlin, 1992.
- [40] R. Manne, Molecular orbital interpretation of x-ray emission spectra - simple hydrocarbons and carbon oxides, *J. Chem. Phys.* 52 (1970) 5733–5739. doi:10.1063/1.1672852.
- [41] R. Kurian, K. Kunnus, P. Wernet, S.M. Butorin, P. Glatzel, F.M.F. de Groot, Intrinsic deviations in fluorescence yield detected x-ray absorption spectroscopy: the case of the transition metal L_{2,3} edges, *J. Phy. Condens. Matter.* 24 (2012) 452201.
- [42] A. Fujimori, F. Minami, Valence-band photoemission and optical absorption in nickel compounds, *Phys. Rev. B.* 30 (1984) 957–971. doi:10.1103/PhysRevB.30.957.
- [43] J. Zaanen, C. Westra, G.A. Sawatzky, Determination of the electronic-structure of transition-metal compounds - 2p x-ray photoemission spectroscopy of the nickel dihalides, *Phys. Rev. B.* 33 (1986) 8060–8073. doi:10.1103/PhysRevB.33.8060.
- [44] A. Kotani, H. Ogasawara, Theory of core-level spectroscopy of rare-earth oxides, *J. Electron Spectros. Relat. Phenomena.* 60 (1992) 257–299. doi:10.1016/0368-2048(92)80024-3.
- [45] L.F. Mattheiss, Electronic Structure of the 3d Transition-Metal Monoxides. I. Energy-Band Results, *Phys. Rev. B.* 5 (1972) 290–306. doi:10.1103/PhysRevB.5.290.
- [46] F.M.F. de Groot, X-ray-absorption and dichroism of transition-metals and their compounds, *J. Electron Spectrosc. Relat. Phenom.* 67 (1994) 529–622. doi:10.1016/0368-2048(93)02041-j.